Subcarrier spacing – a neglected degree of freedom?

Frank Schaich, Thorsten Wild
Alcatel-Lucent AG, Bell Labs Stuttgart, Germany
{frank.schaich, thorsten.wild}@alcatel-lucent.com

***Abstract*—In this paper we assess the pains and potential gains a wireless communication system can leverage on, if we allow for multiplexing different subcarrier spacings within a single transmission time interval (TTI). CP-OFDM is nowadays most often the signal format of choice in wireless communication systems when serving multiple users. LTE/-A, WiFi and WiMAX have all adopted CP-OFDM due to its high degree of flexibility. Though, not all degrees of freedom have been exploited in those systems yet. While these systems are using tailored waveform parameters according to the respective setting – e.g. while WiFi is more tailored towards local area, 4G and WiMAX use settings more suited for wide area – 5G may go one step further by allowing for user specific settings within a single band. With allowing this the signal characteristics may be better matched to the respective channel characteristics such as high Doppler spreads and low coherence times. Our investigations have shown that with exploiting this degree of freedom a higher range of user velocities may be supported, especially with replacing CP-OFDM by UF-OFDM. UF-OFDM modifies the OFDM concept by subband-wise filtering, which mitigates inter-carrier interference (ICI) arising from different parallel subcarrier spacings. This makes it a natural fit for being combined with user-specific subcarrier spacings.**

Keywords—CP-OFDM; UF-OFDM; 5G; subcarrier spacing

I. INTRODUCTION

Multicarrier formats in general and CP-OFDM in particular have proven to be highly flexible in space, time and frequency. If parameterized accordingly, channel estimation/equalization is significantly simplified by allowing for simple one-tap processing in frequency domain. Frequency selective scheduling is enabled allowing for exploiting high gain links while avoiding fading dips. Today's systems successfully exploit many of the degrees of freedom of multi-carrier formats in general and CP-OFDM in particular. However, there is even another potential not yet exploited. While general signal parameters (length of cyclic prefix, subcarrier spacing and connected to this symbol length) are typically chosen to be a reasonable compromise taking the whole range of eventual transmission characteristics (e.g. delay and Doppler spreads) into account, a system allowing for modifying these parameters on a per user basis may allow for significant performance improvements. 5G might be such a system, as it is foreseen that in 2020 a much more diverse set of services request for cellular coverage ([1] and [2]). Additionally, it is foreseen that 5G will have to support a wide range of user velocities. Keeping everything fixed is rarely a good fit to such a big range of transmission characteristics. So, we illustrate in this paper the options we can draw of, if we allow the system to modify the subcarrier spacing on a per user basis (improved channel estimation, improved coverage for power-limited devices, improved support of low latency transmissions; a follow up publication will go into more detail with respect to these). The focus of this paper is on the eventually arising pains and how to cope with them. Receive processing has to be adjusted accordingly, if different parts of the spectrum use different symbol length. Therefore, we additionally investigate means for detection. Naturally, the actual carrier frequency heavily impacts the reasonable region of the subcarrier spacings Δf to be drawn of (e.g. mmW call for much higher spacings than cmW). Here, we concentrate on frequencies below 6 GHz and use Δf = 15 kHz as baseline. To keep it feasible this adaptation applies a code-book approach with 2-4 options (e.g. Δf and $2\Delta f$).

The paper is structured as follows: the next section motivates the paper by providing some insights into the effects we are dealing with and on the potential added values. Then, we introduce our system settings and give some baseline results followed by simulation results indicating potential gains when exploiting configurable subcarrier spacings. Afterwards we present signal processing technologies required for proper detection and conclude the paper.

Notation: We use $(.)^T$ to denote transpose. $\mathbf{0}_{nxm}$ denotes the matrix of size n x m with all zero entries, $\mathbf{I}_n$ the identity matrix of size n. Expectation is denoted by E[.]. Vectors and matrices use bold letters.

II. MOTIVATION

The first question someone has to answer is what improvements are offered to the system with adding this degree of freedom. We see three aspects, here:

- Better support of low latency transmissions
- Improved support of cheap low power nodes
- Improved channel estimation for high speed users. According to [3] velocities up to 500 km/h are expected by NGMN to be supported in 5G.

With 5G some use cases require significantly lower response times. A key element impacting the system latencies is the frame length (in LTE: TTI, transmission time interval). There are two ways to reduce the frame length: (1) reduce the number of symbols and (2) reduce the length of the single symbols. The second point is connected to enabling the use of wider spacings. So, presumably, to achieve very low latencies (up to a factor 10 below LTE) we have to rely on both options – fewer symbols each having shorter duration and thus a wider spacing than the baseline.

978-1-4799-1931-4/15/$31.00 ©2015 IEEE

Another key feature foreseen for 5G is the support of massive machine access. These massive machines are typically low end modules being very cheap and requiring high energy efficiency. So, very low PAPR (peak to average power ratios) is important. Especially, with allocations including only few subcarriers (e.g. 12 equaling a single PRB in LTE covering 180 kHz) PAPR highly depends on the number of subcarriers carrying data. So, with supporting wider spacings low end devices are enabled to achieve a given transmission rate with fewer subcarriers (e.g. with 30 kHz spacing, 6 subcarriers already cover 180 kHz) and thus may benefit from lower PAPR. Additionally, with power constrained devices the power per subcarrier is increased if the allocation only contains 6 subcarriers instead of 12 both improving coverage and transmission rate.

With users moving at speed v and transmitting/receiving signals at carrier frequency f_c we see the following impacts for increasing v:

- Doppler spread is rising leading to intercarrier interference (treated in e.g. [4] and [5]).
- Coherence time of the channel is shrinking leading to lower gains from frequency selective scheduling (not treated here) and to degrading channel estimation quality (assuming a fixed pilot pattern).

This paper covers mainly the very last point, i.e. the impact to the quality of pilot-aided channel estimation. So, in the following we quantify this impact and give means to improve on this.

Assuming Rayleigh fading (following Jakes model) the relation between correlation coefficient and maximum Doppler shift (and related to this the user velocity) can be calculated as follows:

$$\rho(\Delta_t) = J_0(\Delta_t 2\pi f_d) \tag{1}$$

J_0 is the Bessel function of the first kind with 0^{th} order. Δ_t is the time distance between the samples drawn from the process, f_d the maximum Doppler shift with:

$$f_d = \frac{v}{c} f_c \tag{2}$$

c the speed of light. For f_c = 2.5 GHz and various user velocities we get (dotted lines) a correlation as depicted in Figure 1.

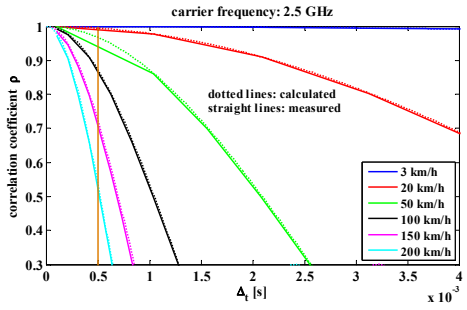

Figure 1: Correlation coefficient ρ between channel realizations at time distance Δ_t for Rayleigh fading (f_c = 2.5 GHz).

The straight lines depicting measured correlations are calculated as follows:

$$\tilde{\rho}(\Delta_t) = \frac{\mathrm{cov}(H_n, H_{n+\Delta_t})}{\sqrt{\mathrm{var}(H_n)\,\mathrm{var}(H_{n+\Delta_t})}} \tag{3}$$

H_n and $H_{n+\Delta t}$ are channel realizations with time distance Δ_t. The vertical line depicts Δ_t = 0.5 ms, i.e. the distance of the reference symbols in the shared data channel (PUSCH) of the LTE uplink (UL). Obviously and as expected, with higher speeds the correlation between channel measurements at this distance is rapidly shrinking, forecasting strong degradations when interpolating the channel between the reference symbols. If users with high velocities would be able to use 30 kHz subcarrier spacing instead of 15 kHz, the actual distance between the reference symbols is halved allowing for performance improvements. Naturally, with higher spacings and thus shorter symbols the impact of delay spread has to be carefully observed (this is the reason, why it is necessary to keep 15 kHz as a baseline and only add 30 kHz as an option instead of fully switching to 30 kHz). In a follow up publication we will investigate these effects in more detail.

III. SYTEM

We very much align our system setup to LTE/-A settings (uplink PUSCH). The baseline subcarrier spacing is Δf = 15 kHz. We start with analyzing SC-FDMA, later we extend to UF-OFDM (applying DFT precoding, too). UF-OFDM is a variation of OFDM applying a per sub-band filter. The following figure depicts a single sub-band (here: 12 subcarriers) both for CP-OFDM and UF-OFDM to indicate the basic difference. A more detailed description of UF-OFDM is available in [6] and [7] and references therein.

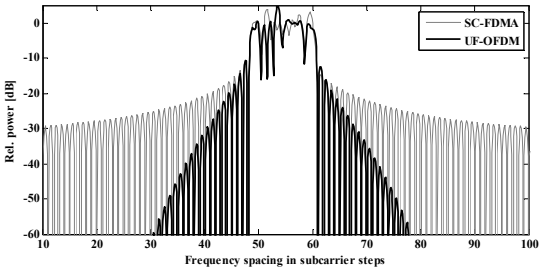

Figure 2: Spectral behavior of SC-FDMA and UF-OFDM.

A single PRB consists of 12 subcarriers and covers thus a width of 180 kHz. Time distance between the reference symbols is 0.5 ms. In this paper we very much focus on the required effort to enable the system to make use of this added degree of flexibility and the impacts to system performance. The actual gains in terms of increased spectral efficiency will be covered in a later publication.

If different spacings share the band, we need separate receiver chains (at digital baseband), being matched to the respective spacing/symbol lengths, respectively. Additionally, we have to provide means to avoid/minimize interference between adjacent allocations applying different spacings.

The signal vector **y** of a single CP-OFDM symbol can be expressed as follows:

$$\boldsymbol{y} = \boldsymbol{\Xi}\boldsymbol{V}\boldsymbol{s}$$
$$\boldsymbol{\Xi} = \left[\left[\boldsymbol{0}_{Lx(N-L)}, \boldsymbol{I}_L\right]^T \boldsymbol{I}_N\right]^T \quad (9)$$

Ξ is a matrix appending the cyclic prefix of length L, **V** is the IDFT matrix with dimension N x N. **s** is the vector with length N containing the complex symbols to be transmitted. If two different spacings are allowed concurrently (e.g. sub-system 1 with Δf_1 = 15 kHz and sub-system 2 with Δf_2 = 30 kHz) the overall system can be viewed as the superposition of two sub-systems each following equation (9) with different N_x and L_x (x = [1, 2]). For compatibility reasons, both sub-systems are to run the same sampling rate. This can be achieved, if the following relation holds:

$$N_1 \cdot \Delta f_1 = N_2 \cdot \Delta f_2 \quad (10)$$

So, we require $N_1 = 2N_2$. Additionally, to have the symbol rate of sub-system 2 to be an integer multiple of sub-system 1 we require: $L_1 = 2L_2$. Then, assuming both systems to be time synchronized and for simplicity leaving out channel coefficient and noise sample, we get the following sum-signal:

$$\boldsymbol{y}_{1\cap 2} = \boldsymbol{y}_1 + \boldsymbol{y}_2$$
$$= \boldsymbol{\Xi}_1\boldsymbol{V}_1\boldsymbol{s}_1 + \begin{bmatrix}\boldsymbol{\Xi}_2\boldsymbol{V}_2\boldsymbol{s}_{2,1}\\ \boldsymbol{\Xi}_2\boldsymbol{V}_2\boldsymbol{s}_{2,2}\end{bmatrix} \quad (11)$$

$\mathbf{y}_{1\cap 2}$ spans a single OFDM symbol of sub-system 1 and two OFDM symbols of sub-system 2 accordingly and has length $N_1+L_1=2(N_2+L_2)$. $\mathbf{s}_1$ carries the symbols to be carried by sub-system 1, $\mathbf{s}_{2,1}$ and $\mathbf{s}_{2,2}$ the ones to by carried by sub-system 2 on the consecutive symbols. $\mathbf{s}_1$, $\mathbf{s}_{2,1}$ and $\mathbf{s}_{2,2}$ are chosen in a way avoiding overlapping main-lobes in frequency domain (i.e. no super-position coding on the same time-frequency resources).

As outlined above we require two distinct demodulators. Let's start with the processing chain being in charge of receiving the 'long' symbols (i.e. the symbols applying 15 kHz spacing in our example namely sub-system 1). So, input to the blocks performing CP removal and FFT is $\mathbf{y}_{1\cap 2}$. Figures 3 and 4 depict the vector at the input of the receiver (both for CP-OFDM and UF-OFDM) schematically (N_1 = 1024, we assume both systems to be time-aligned).

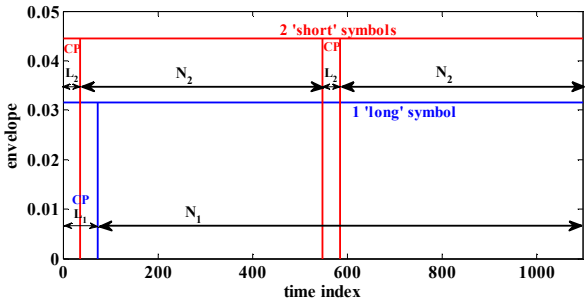

Figure 3: Detector input for sub-system 1 (CP-OFDM). Blue: symbol of interest.

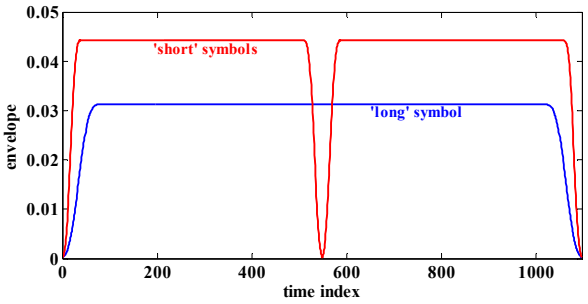

Figure 4: Detector input for sub-system 1 (UF-OFDM). Blue: symbol of interest.

The blue lines depict the samples containing the useful signal for sub-system 1. At the same time these samples carry parts of two consecutive symbols of sub-system 2 (depicted in red). When transforming this to frequency domain, we need to have a closer look to the effects at the boundaries between allocations with different spacings:

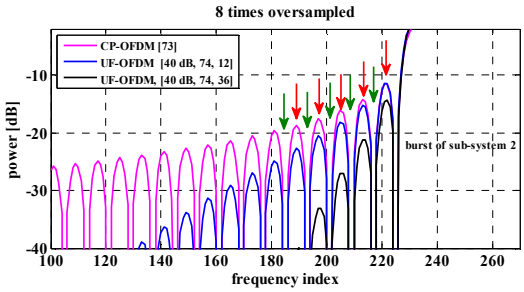

Figure 5: Spectral behavior of sub-system 2 if detected by sub-system 1.

For CP-OFDM we have applied L_1 = 73. The respective UF-OFDM system as described in [6] and [7] applies a filter length of 74 samples (Dolph-Chebyshev filters). Out-of-band attenuation is chosen to be 40 dB. Two different sub-band widths have been investigated (12 and 36 sub-carriers per sub-band). The burst on the right side of Figure 5 carries data being related to sub-system 2. So, the side-lobes being depicted on the left of it have a width of 30 kHz. The arrows indicate the positions of the main-lobes of a burst being associated to sub-system 1, if placed adjacent to the burst being associated to sub-system 2. So, obviously every second main-lobe is confronted with heavy interference and thus would have to be blanked. In case of CP-OFDM this leads to a significant overhead. For UF-OFDM this overhead is small in comparison, due to the much stronger side-lobe level decay of the subband-wise filtering.

The detector for the second sub-system is in charge of detecting the 'short' symbols (i.e. the symbols applying 30 kHz spacing in our example). So, the receiver collects two times N_2+L_2 samples from $\mathbf{y}_{1\cap 2}$ (i.e. collects the two red symbols depicted in Figures 3 and 4, separately). The following figure depicts the vector at the input of the FFT schematically (N_2 = 512, we assume both systems to be time-aligned).

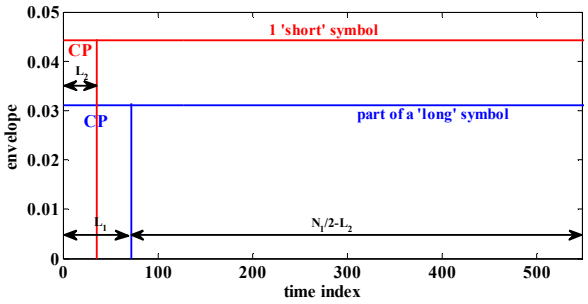

Figure 6: Detector input for sub-system 2 (CP-OFDM). Red: symbol of interest.

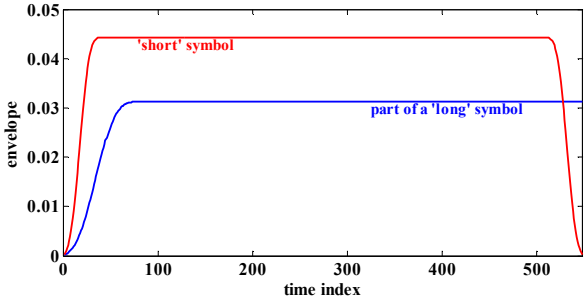

Figure 7: Detector input for sub-system 2 (CP-OFDM). Red: symbol of interest.

Collecting N_2+L_2 samples corresponds to a windowing with a rectangular window having the respective length. Windowing in time domain corresponds to a convolution in frequency domain with the frequency response of the window. The respective impact to sub-system 1 is as follows.

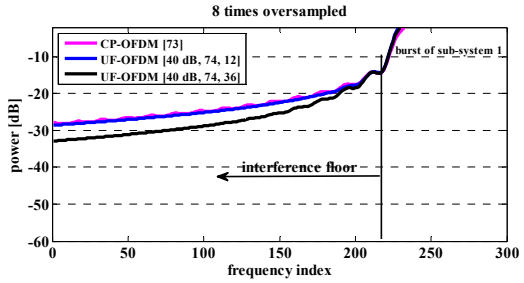

Figure 8: Spectral behavior of sub-system 1 if detected by sub-system 2.

Obviously, heavy interference is introduced, if we apply rectangular windows. Though, we have investigated alternatives.

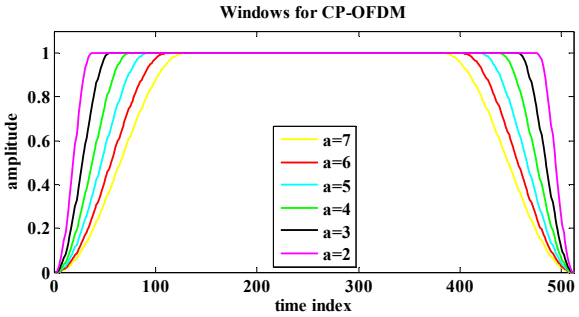

Figure 9: Receive windows CP-OFDM.

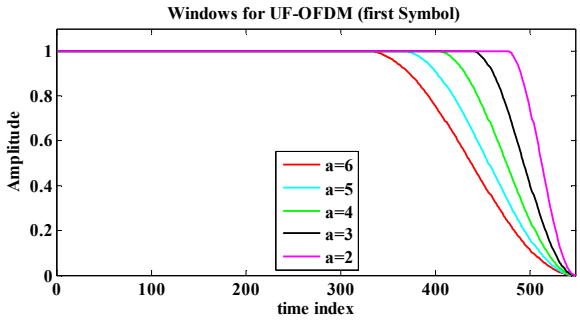

Figure 10: Receive windows UF-OFDM.

Instead of rectangular windows, we apply windows with raised-cosine shaped edges. a is the so-called ramp-width factor. The actual width (in number of samples) of the ramp is aL_2. Assuming the sub-systems to be time-aligned the window for detecting UF-OFDM only requires a ramp at one side of the window, thanks to the ramps of the transmit symbols (see Figure 7), stemming from the basic time domain properties of UF-OFDM. Figure 10 depicts the respective windows for receiving the 'first' short symbol within $\mathbf{y}_{1\cap 2}$. For detecting the 'second' symbol the ramp would have to be at the beginning of the window. If the two sub-systems are not time-aligned both ends of the window would have to include a ramp.

Applying any of these windows has two impacts:

- The intercarrier interference floor is reduced.
- Self-interference is introduced.

We have analyzed both effects. The following figures depict the achieved reduction of the error floor for various values of a:

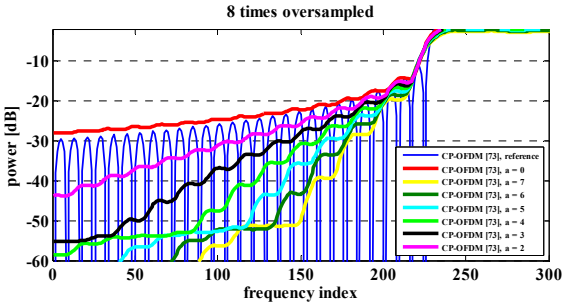

Figure 11: Interference floor reduction (CP-OFDM)

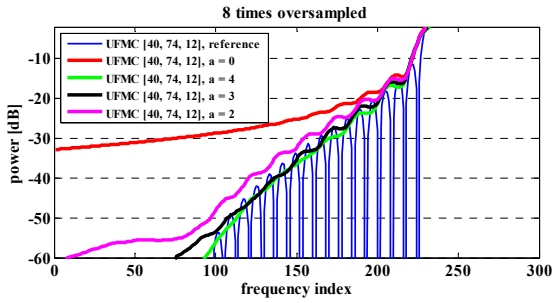

Figure 12: Interference floor reduction (UF-OFDM, 12 subcarriers per sub-band).

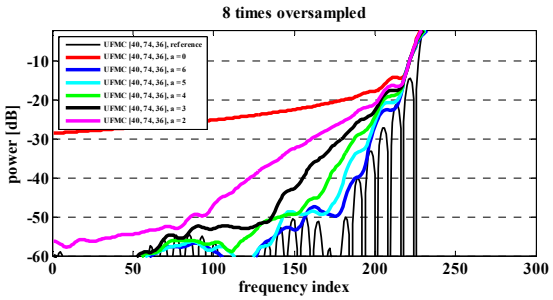

Figure 13: Interference floor reduction (UF-OFDM, 36 subcarriers per sub-band).

Obviously, the interference floor can be kept under control by applying the windows. Though, with UF-OFDM we can use a less aggressive ramp-width factor a. While for UF-OFDM $a = 2$ and $a = 4$, respectively, are sufficient to keep the floor low, CP-OFDM requires $a = 7$.

The second effect is the introduction of self-interference. The following figure depicts this effect for the three cases (CP-OFDM, UF-OFDM12 and UF-OFDM36) depending on the ramp-width factor. Additionally, the capability of zero-tail DFT spreading [8] to combat this distortion is shown.

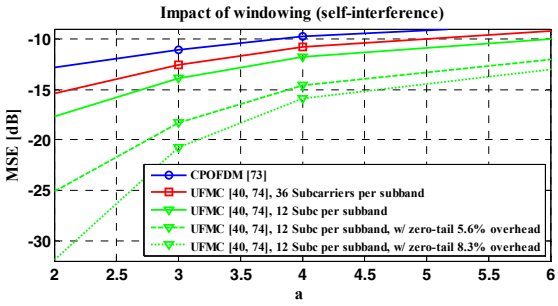

Figure 14: Self-interference (in dB) due to non-rectangular receive windowing.

Obviously, CP-OFDM is more sensitive to this, especially, as CP-OFDM requires higher ramp-width factors.

IV. Conclusions

We have analyzed a LTE-like system, whether supporting adaptable subcarrier spacings on a per user basis can bring sufficient gains and if potential pains (e.g. self-interference) can be kept in check. While systems applying either CP-OFDM or UF-OFDM can harvest on significant gains by better supporting a high range of user velocities, UF-OFDM is to be preferred as UF-OFDM better copes with the arising pains. With UF-OFDM we only have to invest very few subcarriers as guards between the different zones (I.e. different spacings should not be completely intermixed. Instead we propose to use different zones supporting different spacings, respectively. To follow different user mixes during the course of a day resources between the zones may be traded on a regular base). Additionally, CP-OFDM introduces significant self-interference at the receiver, while for UF-OFDM the amount of self-interference is negligible. So, as a consequence a system applying UF-OFDM is able to support different spacings concurrently within a single band opening the option for implementing a code-book based adaptation mechanism to improve the support of different user speeds more efficiently and to enable the system to support low latency modes and low end devices more efficiently.

This publication mainly covers the pains the system would have to cope with (for supporting the flexibility related to subcarrier spacing) and only indicates the potential gains. A follow up publication will more deeply investigate the gains and compare to alternative approaches (e.g. keeping the spacing while increasing pilot density in time direction).

References

[1] Wunder, G.; Jung, P.; Kasparick, M.; et al., "5GNOW: non-orthogonal, asynchronous waveforms for future mobile applications," *Communications Magazine, IEEE*, vol.52, no.2, pp.97,105, February 2014.

[2] Osseiran, A.; Braun, V.; Hidekazu, T.; et al., "The Foundation of the Mobile and Wireless Communications System for 2020 and Beyond: Challenges, Enablers and Technology Solutions," *Vehicular Technology Conference (VTC Spring), 2013 IEEE 77th* , pp.1,5, 2-5 June 2013.

[3] NGMN white paper, "A deliverable by the NGMN Alliance", February 2015.

[4] Schellmann, M.; Zhao, Z.; Lin, H.; Siohan, P.; Rajatheva, N.; Luecken, V.; Ishaque, A., "FBMC-based air interface for 5G mobile: Challenges and proposed solutions," *Cognitive Radio Oriented Wireless Networks and Communications (CROWNCOM), 2014 9th International Conference on* , pp.102,107, 2-4 June 2014.

[5] Fuhrwerk, M.; Peissig, J.; Schellmann, M., "Channel adaptive pulse shaping for OQAM-OFDM systems," *Signal Processing Conference (EUSIPCO), 2014 Proceedings of the 22nd European*, pp.181,185, 1-5 Sept. 2014.

[6] Schaich, F.; Wild, T., "Relaxed synchronization support of universal filtered multi-carrier including autonomous timing advance," *Wireless Communications Systems (ISWCS), 2014 11th International Symposium on* , pp.203,208, 26-29 Aug. 2014.

[7] Wild, T.; Schaich, F.; Chen, Y., "5G air interface design based on Universal Filtered (UF-)OFDM," *Digital Signal Processing (DSP), 2014 19th International Conference on*, pp.699,704, 20-23 Aug. 2014.

[8] Berardinelli, G.; Tavares, F.M.L.; Sorensen, T.B.; Mogensen, P.; Pajukoski, K., "Zero-tail DFT-spread-OFDM signals," *Globecom Workshops (GC Wkshps), 2013 IEEE*, pp.229,234, 9-13 Dec. 2013.